Vital Signs Monitoring with a UWB Radar Based on a Correlation Receiver

Mario Leib*,Wolfgang Menzel*, Bernd Schleicher†, and Hermann Schumacher†

*Ulm University, Microwave Techniques, Albert-Einstein-Allee 41, 89081 Ulm, Germany
†Ulm University, Electron Devices and Circuits, Albert-Einstein-Allee 45, 89081 Ulm, Germany
Email: mario.leib@uni-ulm.de

***Abstract*—In the first part of this publication, vital signs detection observing small amplitude changes due to the movement of a target in front of the radar is shown. In the context of vital signs monitoring the target is the chest of human beings. This basic principle is also used in continuous wave (CW) radars, but the presented impulse-based UWB radar has moreover a range gating capability. Consequently, the target distance can be obtained and different targets (persons) can be monitored. Several measurement results using this measurement principle for respiration and in particular for heart beat monitoring are presented and discussed. Furthermore, the shortcomings of this method are depicted.**

In the second part, advanced signal post-processing by deconvolution with a Wiener filter is presented, leading to an improved resolution performance for the realized UWB radar system. Promising results of this method show that small targets can be identified in a multi-target scenario. Therefore, the movement of small targets, e. g. the heart muscle within the human body, could be tracked directly.

***Index Terms*—ultra-wideband (UWB), radar, impulse radio, vital signs monitoring, medical application**

I. Introduction

Due to the inherent ultra-wide bandwidth, UWB radar technology offers the possibility for high-resolution measurements. In combination with the low-power consumption of impulse-based systems and the low radiated power levels, UWB is in particular attractive in the medical environment. Potential applications in this field go from breast cancer detection [1], [2], aortic pressure measurement [3], hip prosthesis identification [4] to vital signs (respiration and heart beat) measurement [5]. The latter could be applied for a remote electrocardiogram useful for a convenient observation of patients [6], for burned victims, where no sensor can be attached to the human body, or for home monitoring systems, where, for example, the sensors are integrated in the clothing using smart textiles [7]. As the radar measures the actual position variations of the heart muscle instead of the electrical pulses exciting the heart, this could be also used for the compensation of organ movements in computer tomography for improved imaging [8].

This paper deals with the measurement of the vital signs of human beings using a correlation based UWB radar. After a brief introduction of the sensor, the focus is on the measurement results and the challenges of determining the heart beat signal. Finally, a method for resolution improvement is presented, based on the deconvolution of the radar system impulse response using a Wiener filter.

II. UWB Radar System

The complete ultra-wideband radar system consists of a bistatic front-end with separated transmitter and receiver, an electronic unit with power supply and controlling circuitry, and a laptop for data visualization (see Fig. 1). The basic elements of the transmitter and the receiver are a planar tapered slot antenna [9] and an impulse generator (IG) creating a 1st derivative Gaussian impulse shape [10]. The spectrum of the impulse is almost compliant with the FCC frequency mask reaching from 3.1 GHz to 10.6 GHz. In the receiver, the correlation concept is implemented using a mixer and a reference impulse generator with the same impulse shape as in the transmitter. A simplified block diagram of the overall system is shown in Fig. 2. More details about the radar systems and its key components can be found in [11].

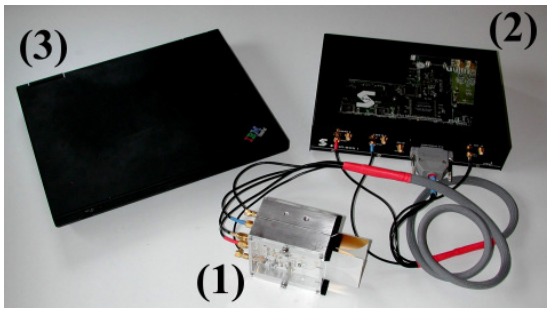

Fig. 1. Complete UWB radar sensor system with front-end (1), electronic unit (2) and laptop (3).

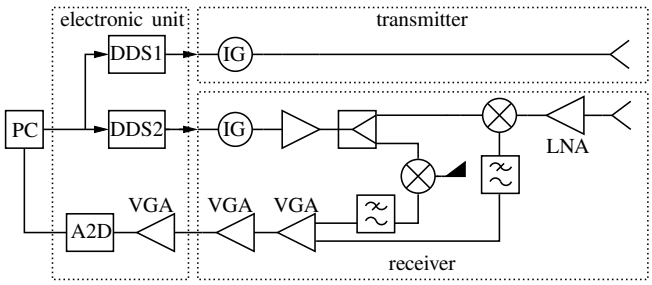

Fig. 2. Block diagram of the UWB radar system.

III. Vital Signs Detection

A. Operation Principle

The area in front of the radar is scanned changing the time delay of the reference impulse in the receiver in comparison to the transmitted impulse. This is applied adjusting the phase of the reference impulse generator's clock signal. If an impulse is reflected at a target, the correlation function between the transmit and receive impulse is obtained. The position of the maximum of the correlation function corresponds to the actual target distance.

In order to determine the movement of a target, the target position can be recorded over time. For small position variations in the centimeter range — like for breathing and heart beat — a more convenient method can be applied with the correlation receiver. If the time delay of the reference impulse is fixed to the position of a target, then any movement will change the output amplitude of the receiver. As the relationship between the target distance and the output amplitude is almost linear around the maximum of the correlation function, a distance change is proportional to the output amplitude of the sensor. Therefore, small movements of a target can be directly observed by the output signal of the receiver.

This method is also used in CW radars in order to measure small movement variations and in particular the respiration and heart beat of humans [12]. However, the position of a target cannot be distinguished there. So, if many moving targets are in the field of view, the movements cannot be assigned to a certain target in contrast to the UWB radar.

B. Validation of Operation Principle

In Fig. 3 the output voltage of the UWB radar is shown, when the radar is directed towards the sternum of a human and the distance is fixed to the skin-air boundary. The breathing of the person with a breath hold of 12 s at 35 s can be clearly seen there. The breathing rate of 23.4 breaths/min (0.39 Hz) is obtained applying the Fourier transformation (see. Fig. 4).

With this setup the heart beat of a slim test person is also detectable because shock waves created by the heart lead to a slight movement of the outer skin. This is indicated during the breath-hold phase by the small ripples with a higher frequency than the breath rate. In the overall spectrum, the heart beat rate is not visible due to the low amplitude caused by the low movement of the outer skin by the heart beat. But, if a bandpass filter is applied suppressing the breathing frequency, the heart beat with a rate of 56 beats/min (0.93 Hz) is obtained. This value is confirmed by a synchronous measurement with an electrocardiograph (ECG) [13]. In the frequency domain, exactly the same heart beat rate is obtained, as shown in Fig. 4. Furthermore, the time domain signal, presented in Fig. 5, shows a good agreement between the ECG signal and the filtered radar signal. Please keep in mind that the electrocardiograph measures the electrical signal stimulating the heart muscle, whereas the radar measures the actual movement of the heart muscle.

C. Discussion and Shortcomings

Due to the strong reflection at the air-skin boundary, the respiration of a person can be measured easily with the described method as far as the person does not move during the data acquisition. In this case, an inconvenient tracking to the air-skin boundary is needed. As shown, the heart beat rate can also be determined applying a bandpass filter. The detection and measurement of the heart beat is possible in the presented example because of the movement of the chest of a slim test person. For more corpulent persons the heart beat rate could be also determined, but the amplitude is even smaller as the outer tissue layers of the chest are hardly excited by the heart's shock waves. Hence, the detection is more challenging.

Furthermore, measurements of persons with different constitutions, heart beat rates and breathing behavior showed that harmonics generated by the breathing signal in combination with the non-linear correlation function can lead to ambiguous

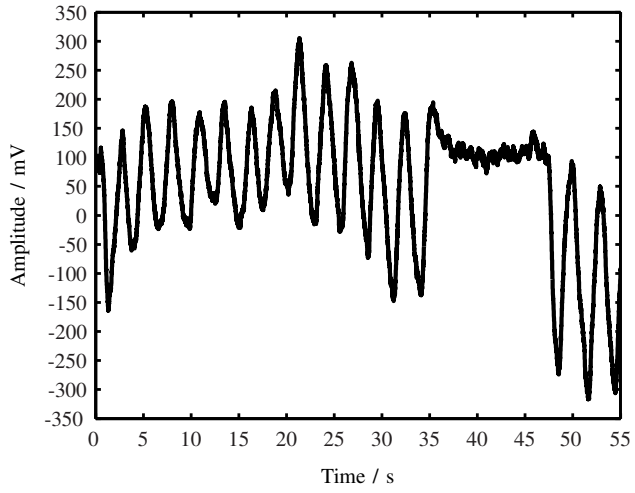

Fig. 3. Measured sensor output for a breathing person and a breath hold of about 12 s.

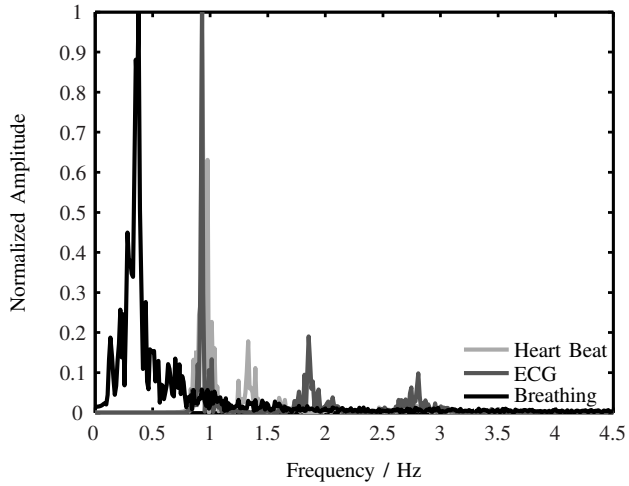

Fig. 4. Normalized spectrum of the recorded breathing and heart beat signal in Fig. 3 using a bandpass filter and comparison with the spectrum recorded with an ECG.

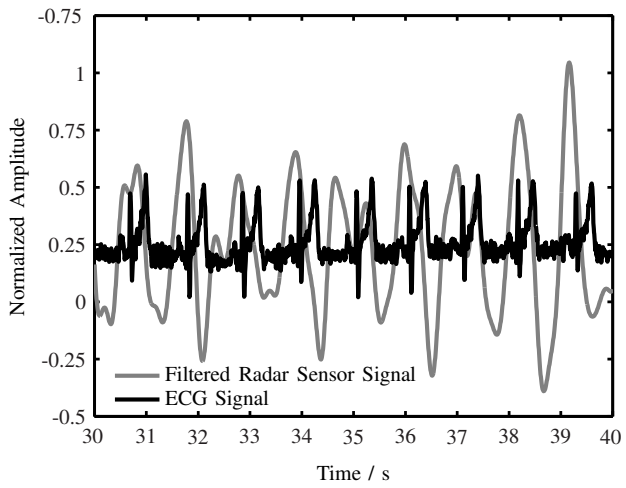

Fig. 5. Comparison of the filtered sensor output from Fig. 3 with the synchronously recorded ECG signal.

results. Especially in case of deep respiration, the level of the harmonics can be equal or even higher than for the heart beat signal with its low amplitude in time domain. For instance, Fig. 6 presents the measured spectrum for a person after some sporting activity. The breath rate of $f_\mathrm{b} = 0.48\,\mathrm{Hz}$ and the first harmonic can be clearly seen. A bandpass filter with a pass band between 1.1 Hz and 4 Hz is applied to separate the heart beat from the breathing signal. If only the filtered spectrum for the heart beat rate is observed, a value of 1.44 Hz (86.4 beats/min) could be misleadingly deduced. However, that is the third harmonic of f_b. A notch filter canceling the harmonics of the breathing signal as proposed in [14] is a suitable countermeasure and is applied in Fig. 7. As confirmed by a synchronous ECG measurement, the proper heart beat rate of 1.68 Hz (101 beats/min) is observed then. This method fails if the heart beat rate is a multiple of the breathing rate. In summary, reliable measurements of the heart beat rate without any reference is only possible in case of a breath hold or at least at weak respiration and no body movements. This, however, limits the application of this method to narcotized patients.

IV. Resolution Improvement based on Deconvolution with a Wiener Filter

As already mentioned, a different method to measure movements would be the tracking of a certain target. Since the transmitted radar signal penetrates into the human body and the boundary between the heart muscle and since the surrounding fat tissue has a significantly different permittivity, the heart could be detected and its movements monitored. Currently, however the monitoring of the heart muscle is unfeasible as the signal is strongly attenuated and therefore disappears within the ringing signal of the main target, the skin-air boundary. This ringing is caused by the transmit impulse itself and the non-ideal effects of the radar systems, e. g. multiple reflections at discontinuities and mismatch. In the following, an approach is described to distinguish between several targets with different radar cross sections, e. g. like the chest and heart muscle for the vital signs monitoring.

The output signal of the UWB radar for a single target and two laterally shifted targets is shown in Fig. 8. The single target T_1 is a metal plate located 70 cm in front of the radar. Although the radar response shows a strong ringing behavior, the target position is clearly detectable by the minimum value of the obtained correlation signal. The minimum needs to be observed, since the metal plate performs a phase change of 180°. In the two-target scenario, a large metal plate T_{21} is placed at a distance of 40 cm and a small metal plate T_{22} with a lower radar cross section is positioned 44.5 cm away. The large metal plate is once again clearly detectable, but the

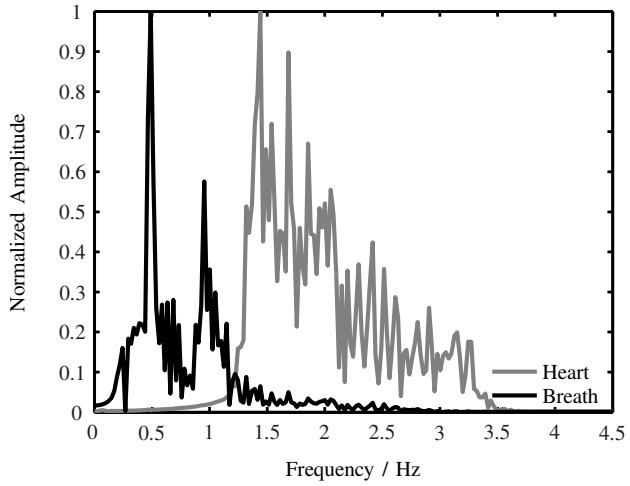

Fig. 6. Normalized spectrum for the measurement of a person after some sporting activities. A bandpass filter is applied to separate the breathing and the heart beat (1.1 Hz-4 Hz).

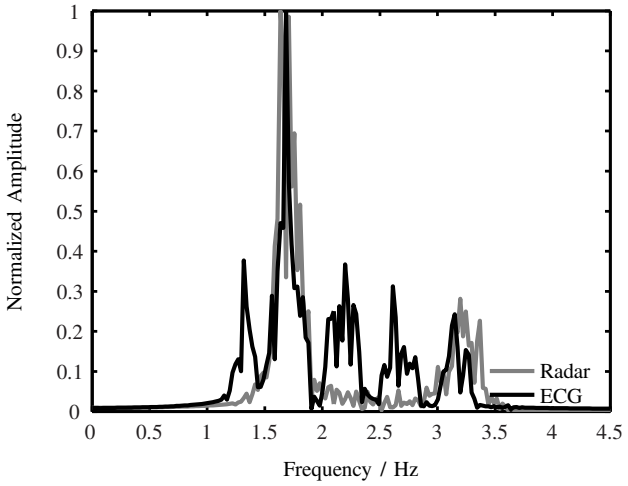

Fig. 7. Spectrum of the bandpass filtered heart beat signal in Fig. 6 after applying an additional second order notch filter in comparison with the spectrum recorded with an ECG.

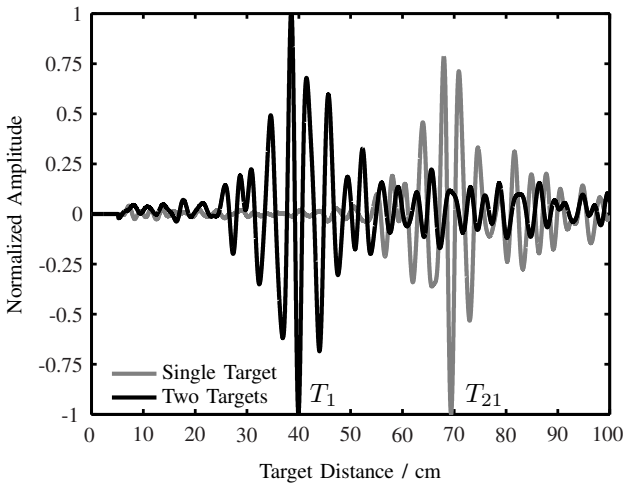

Fig. 8. Measured sensor output for a single target (metal plate) at $x_1 = 70$ cm and two targets ($x_{21} = 40$ cm, $x_{22} = 44.5$ cm) with different radar cross sections.

second target disappears within the correlation signal of the large metal plate and cannot be observed.

In order to be able to detect small targets increased resolution performance is required. This can be performed by deembedding all time-invariant influences of the radar system. Therefore, the impulse response $h_{\mathrm{SYS}}(t)$ of the radar system is determined by a separate measurement using a non-resonant reference target at a known position R. A flat metal plate covering the whole antenna main beam is such a suitable reference target. The radar system can be described in a system theoretical way for the calibration measurement as illustrated in Fig. 9. Then, the system impulse response $h_{\mathrm{SYS}}(t)$ can be calculated reversing the correlation operation, deconvoluting the transmit signal $s_{\mathrm{IN}}(t)$, and compensating the delay by the known target distance. To this end, the reference signal $s_{\mathrm{REF}}(t)$ within the receiver and the transmit signal $s_{\mathrm{IN}}(t)$ must be available. Finally, the hereby obtained system impulse response can be compensated from the radar response $s'_{\mathrm{OUT}}(t)$

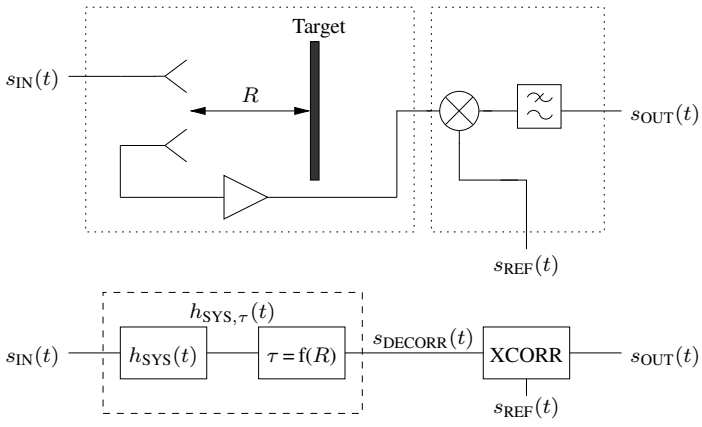

Fig. 9. Simplified block diagram of the UWB radar system (top) and mapping to its system theoretical description (bottom).

1.) Determination of the System Impulse Response (Calibration)

Decorrelation:
$s_{\mathrm{DECORR}}(t) = \mathrm{deconv}(s_{\mathrm{REF}}(-t), s_{\mathrm{OUT}}(t))$

Deconvolution of the Input Signal:
$h_{\mathrm{SYS},\tau}(t) = \mathrm{deconv}(s_{\mathrm{DECORR}}(t), s_{\mathrm{IN}}(t))$

Delay Compensation of the Reference Target:
$h_{\mathrm{SYS}}(t) = h_{\mathrm{SYS}}(t+\tau)$

2.) Compensation of the System Impulse Response

Decorrelation:
$s'_{\mathrm{DECORR}}(t) = \mathrm{deconv}(s_{\mathrm{REF}}(-t), s'_{\mathrm{OUT}}(t))$

Deconvolution of the System Impulse Response:
$s'_{\mathrm{OUT,\,DECONV}}(t) = \mathrm{deconv}(s'_{\mathrm{DECORR}}(t), h_{\mathrm{SYS}}(t))$

Deconvolution of the Input Signal:
$s'_{\mathrm{OUT},\delta}(t) = \mathrm{deconv}(s'_{\mathrm{OUT,\,DECONV}}(t), s_{\mathrm{IN}}(t))$

Fig. 10. Flowchart for the determination of the system impulse response h_{SYS} using a reference target at known position R (τ) and the compensation of h_{SYS} for an output signal s'_{OUT} without any target information.

of another measurement with an unknown target scenario. The whole mathematical procedure for the calibration and the application to a radar response is summarized in the flowchart in Fig. 10. The inevitable deconvolution operation *deconv()* is performed in the frequency domain with a first order Wiener filter $W(f)$ [15], where the signal-to-noise ratio (SNR) is determined empirically for each deconvolution process:

$$W(f) = \frac{S^*_{\mathrm{IN}}(f)}{|S_{\mathrm{IN}}(f)|^2 + \mathrm{SNR}}, \quad (1)$$

$$H_{\mathrm{SYS}}(f) = W(f) \cdot S_{\mathrm{OUT}}(f). \quad (2)$$

Fig. 11 shows the results after applying the described signal processing to the scenario with one and two targets (compare Fig. 8). The large targets (T_1, T_{22}) are more clearly observable and even the small target T_{22} in the two-targets case can be detected. In addition, the ground reflections (G_1, G_2) are visible at 53 cm and 84 cm, respectively.

In general, a Dirac-like response is obtained instead of a broad correlation function applying this signal processing, whereas the width of the response and hence the resolution limit is related to the effective bandwidth of the UWB radar system. Practical evaluation showed a resolution limit of about 2 cm, which is in accordance with the approximated 10 dB system bandwidth of 7 GHz.

Finally, a wooden board with a thickness of 17 mm with an unknown dielectric constant is used as target in order to investigate the capabilities of the UWB radar to look inside bodies. In Fig. 12 the post-processed radar output signal is shown for the board. The reflections of the electromagnetic wave at the beginning T_{31} and the end T_{32} of the board can be detected. The amplitude of T_{32} is lower than for T_{31} due

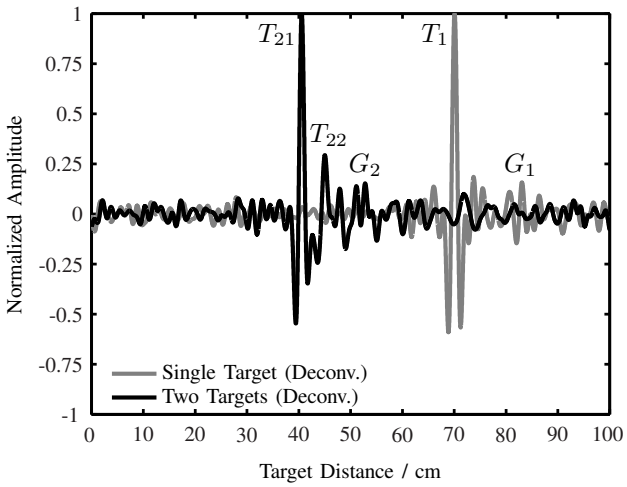

Fig. 11. Output signal of the raw data presented in Fig. 8 after application of the described deconvolution method.

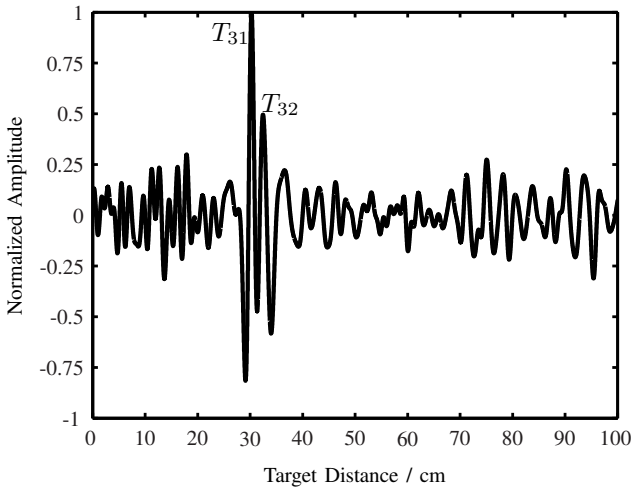

Fig. 12. Output signal after signal post-processing for a wooden board with a thickness of 17 mm as target.

to the material loss of wood. Although the board thickness is lower than the resolution limit, both reflections can be detected since the propagation velocity within wood is lower than in air. Hence, the distance between the reflections is 21.8 mm instead of 17 mm. This can be used to calculate the relative permittivity ε_r of the board. The obtained value of $\varepsilon_\mathrm{r} = 1.6$ explains the low amplitude of the reflections, since, therefore, the wave mainly penetrates the board instead of being reflected. In conclusion, it can be stated that it is possible to look into bodies using the deconvolution method. However, the detection of the heart within the human body is still challenging due to the complex environment and the high attenuation of human tissue. With the described UWB radar, the heart could not been detected due to the low transmit power and the low directivity of the antenna.

V. Conclusion

This paper shows that respiration and heart beat of persons can be measured with a UWB correlation radar. However, some challenges occur for heart beat measurements with the described method limiting it to specific applications. In addition, an approach to detect a target with a low radar cross section within the response of the UWB radar is introduced. This method shows promising results and is also beneficial for imaging systems.

Acknowledgment

This work has been funded by the German Research Foundation (DFG) under the program UKoLoS.

References

[1] S. K. Davis, B. D. V. Veen, S. C. Hagness, and F. Kelcz, "Breast tumor characterization based on ultrawideband microwave backscatter," *IEEE Transactions on Biomedical Engineering*, vol. 55, no. 1, pp. 237–246, Jan. 2008.

[2] M. Klemm, I. J. Craddock, J. Leendertz, A. W. Preece, and R. Benjamin, "Breast cancer detection using symmetrical antenna array," in *European Conference on Antennas and Propagation*, Nov. 2007.

[3] L. E. Solberg, I. Balasingham, S.-E. Hamran, and E. Fosse, "A feasibility study on aortic pressure estimation using UWB radar," in *IEEE International Conference on Ultra-Wideband*, Sep. 2009, pp. 464–468.

[4] H.-S. Lui, N. Shuley, and S. Crozier, "A concept for hip prosthesis identification using ultra wideband radar," in *IEEE Engineering in Medicine and Biology Society Conference*, vol. 1, Sep. 2004, pp. 1439–1442.

[5] M. Chia, S. Leong, C. Sim, and K. Chan, "Through-wall UWB radar operating within FCC's mask for sensing heart beat and breathing rate," in *European Radar Conference (EURAD)*, Oct. 2005, pp. 267–270.

[6] K. Higashikaturagi, Y. Nakahata, I. Matsunami, and A. Kajiwara, "Non-invasive respiration monitoring sensor using UWB-IR," in *IEEE International Conference on Ultra-Wideband*, vol. 1, 2008, pp. 101–104.

[7] T. Kellomaki, W. G. Whittow, J. Heikkinen, and L. Kettunen, "2.4 GHz plaster antennas for health monitoring," in *European Conference on Antennas and Propagation*, Mar. 2009, pp. 211–213.

[8] F. Thiel, M. Hein, U. Schwarz, J. Sachs, and F. Seifert, "Fusion of magnetic resonance imaging and ultra-wideband-radar for biomedical applications," in *IEEE International Conference on Ultra-Wideband*, vol. 1, 2008, pp. 97–100.

[9] P. Gibson, "The Vivaldi aerial," in *European Microwave Conference (EuMC)*, Oct. 1979, pp. 101–105.

[10] J. Dederer, C. Schick, A. Trasser, and H. Schumacher, "A SiGe impulse generator for single-band ultra-wideband applications," *Semiconductor Science and Technology*, vol. 22, no. 1, pp. 200–203, Jan. 2007.

[11] M. Leib, E. Schmitt, A. Gronau, J. Dederer, B. Schleicher, H. Schumacher, and W. Menzel, "A compact ultra-wideband radar for medical applications," *Frequenz*, vol. 63, no. 1-2, pp. 1–8, Feb. 2009.

[12] M. Jelen and E. M. Biebl, "Multi-frequency sensor for remote measurement of breath and heartbeat," *Advances in Radio Science*, vol. 4, pp. 79–83, 2006.

[13] M. Cremmel, "GBEKG ," *Elektor*, no. 10, pp. 32–41, Oct. 2006.

[14] A. Lazaro, D. Girbau, and R. Villarino, "Analysis of vital signs monitoring using an IR-UWB radar," *Progress In Electromagnetics Research (PIER)*, vol. 100, pp. 265–284, 2010.

[15] S. V. Vaseghi, *Advanced Signal Processing and Digital Noise Reduction*. New York, USA: John Wiley & Sons Ltd., 1996.